Supplementary materials to '**A hydromorphic re-evaluation of the forgotten river civilizations of Central Asia**'

S1: Extended cultural and hydroclimatic setting for the Otrār oasis

S1.1: Historical and archaeological setting development of Otrār oasis and the Syr Darya valley
During the Bronze Age the Syr Darya valley and surrounding steppes were inhabited by people of the the Andronovo culture (ca. 2000 - 900 BCE)[1]. In the early 1st millennium BCE, the region became dominated by the nomadic Scythian confederacy of the Saka who controlled the region between the Caspian Sea, the Pamir Mountains and the Tarim Basin[1-3]. Transoxania came under Achaemenid Rule during the 6th century BCE, with the Syr Darya River forming the northeastern border of the Achaemenid Empire[3,4]. The Achaemenid Period (ca. 550 - 330 BCE) marks the emergence of urban centers in Transoxania and the establishment of large-scale floodwater irrigation systems in the Syr Darya basin, and particularly in the lower reaches and delta of the Amu Darya (Khorezm)[1,5].

Hellenic Rule over the the Syr Darya basin commenced with conquest by Alexander the Great (329 BCE), continued with Hellenic successor states such as the Greco-Bactrian Kingdom, and ended with the invasions of nomadic tribes from the Central Asian steppes during the 2nd century BCE. The migration of nomadic tribes into Transoxania is generally attributed to the expansion of the Xiongnu Empire in the Mongolian region during the late 3rd century BCE. This triggered a cascade of migration by Yuezi, Wusun and Kangju people, each forcing the previous inhabitants out of the region (starting with the Saka)[3].

During the mid- to late-3rd century CE Transoxania became part of the Sassanid Empire, again with its northeastern border located at the Syr Darya River. Sassanid control was relatively short-lived and ended with the incursions of Hunnic tribes (e.g. the Kiderites, Xionites and Hephtalites)[6-8], who established nomadic kingdoms from the mid- to late-4rd century CE onwards. The Göktürks invaded Transoxania from the northeast during the mid-6th century CE, and the region became part of a series of Göktürk Khaganates, which persisted until the Arab invasions of the mid-8th century CE[3,6,9,10].

The foundation of Otrār and many urban sites in the Syr Darya valley date to the early 2nd century BCE (Kangju period). Later these were fortified during the rule of nomadic Turkic princedoms[11] in order to protect the main Silk Road caravan route that ran past Taraz and between Transoxania in the west and China in the east. Similar to the city of Otrār, the other large settlements in the oasis (e.g. Kuik Mardan, Kok Mardan, Jalpak(tobe), Altyn(tobe), Kuyruk(tobe)) covered an area of at least ca. 12 ha^2 and are characterized by a high flat-topped mound, known locally as a tobe or tell. They were typical of Central Asian cities with a basic tripartite structure of citadel, fortified inner town (shakhristan) and suburbs (rabad), with the administrative authorities and military based within the citadel and inner town, and lower status housing and industrial manufacturing located outside the town walls[12,13].

S1.2: Regional climatic framework
Climate variability over Central Asia is largely controlled by the intensity of mid-latitude Westerlies. Depressions that develop over the eastern part of the Mediterranean and regenerate over the Caspian Sea region transport moist air to Central Asia[14,15]. The region is shielded by the high Pamir and Tien Shan Mountains from monsoonal influences from the southeast[15]. Precipitation over the Aral Sea basin, including the Syr Darya catchment, is controlled by the shifts of the westerly cyclonic circulation. Primary teleconnections are suggested with strength of the Siberian High[16,17], whose strength and location influences the latitudinal position of storm tracks and their eastward extent, with the potential to protrude as far as the eastern Mongolian Plateau[18]. Rainfall over mid-latitudes of Central Asia has been shown to be related to changes in the mode of the North Atlantic Oscillation

(NAO), being high during a negative NAO mode with increased cyclonic activity over the eastern Mediterranean[19].

S2: The dating of Otrār oasis canal-fill deposits

S2.1 The sedimentology of canal fills

Ancient irrigation canals were surveyed using satellite imagery[20] to locate main feeder canals running up to fortified settlements and agricultural zones of Otrār oasis. Narrow trenches, with a width of ca. 1m and reaching down to the local clay substrate at 2-3m depth, were dug using a mechanical excavator either across the entire abandoned canal feature or, where this was not possible, ran from one edge towards its center. Overall canal dimensions such as the width, depth, and geometry of all excavated canals were recorded as well as the height and shape of bounding banks. The infill of each canal was logged and consistently four sedimentary units were found (Fig. S1). Unit A is a densely packed blue-grey clay substrate that marks the bottom of the canals, and is located between 2 - 3 meters from present ground level. The origin and spatial extent of the basal clay substrate remains to be investigated, but its formation is believed to be either the distal facies of an inland delta of the Arys river, deposited prior to the Achaeminid Period[21], or a lacustrine deposit in a regional depression, deriving its water and sediment from periodic Syr Darya flooding. Unit B is formed of cross-bedded fine sands at the base of the irrigation canals, of a thickness between 20-50 cm. A sharp erosional contact with the lower unit A and the occurrence of clayey rip-up clasts indicates that this unit represents a phase of active flow within the canal. In Trench 4 similar deposits form part of a later infill, during a period of canal reactivation. Unit C and D were formed by siltation of irrigation canals and abandonment. Unit C ranges in texture from sandy silt to silt, is fining upward and marked by horizontal bedding and includes ceramic fragments and charcoal. At most investigated sections, Unit D formed the upper part the canal fill and consists of uniform silty clays. It marks the final stage of canal infilling under stagnant water conditions. Unit D was often observed to be thicker in the central part of the abandoned canal fill.

With the exception of Trench 6, all samples for dating canal abandonment were taken from Unit C, which formed as the irrigation system was falling into disuse. Previous studies have indicated that samples from the very base of irrigation canals may represent the active phase rather than abandonment[22,23]; therefore, unit B was avoided for sample collection. The horizontally bedded lithofacies of Unit C were targeted for dating, as these represent deposits formed by successive passage of pulses of water and sediment under conditions of decreasing flow in the canal during the early stages of abandonment[24]. There is no evidence of post-depositional disturbance of Unit C by digging, in order to clean or re-cut the canal, indicating that OSL and ^{14}C ages from this unit provide the most accurate dates for canal abandonment. Dating of Unit D was considered to be less appropriate for constraining canal abandonment, as local ponding in defunct canal depressions could have occurred for a prolonged period after the irrigation system went out of use. High-intensity precipitation events can mobilize material on the banks of the canal and the age reversal evident in Trench 6 is believed to be the result of old charcoal being washed into the canal long after its abandonment.

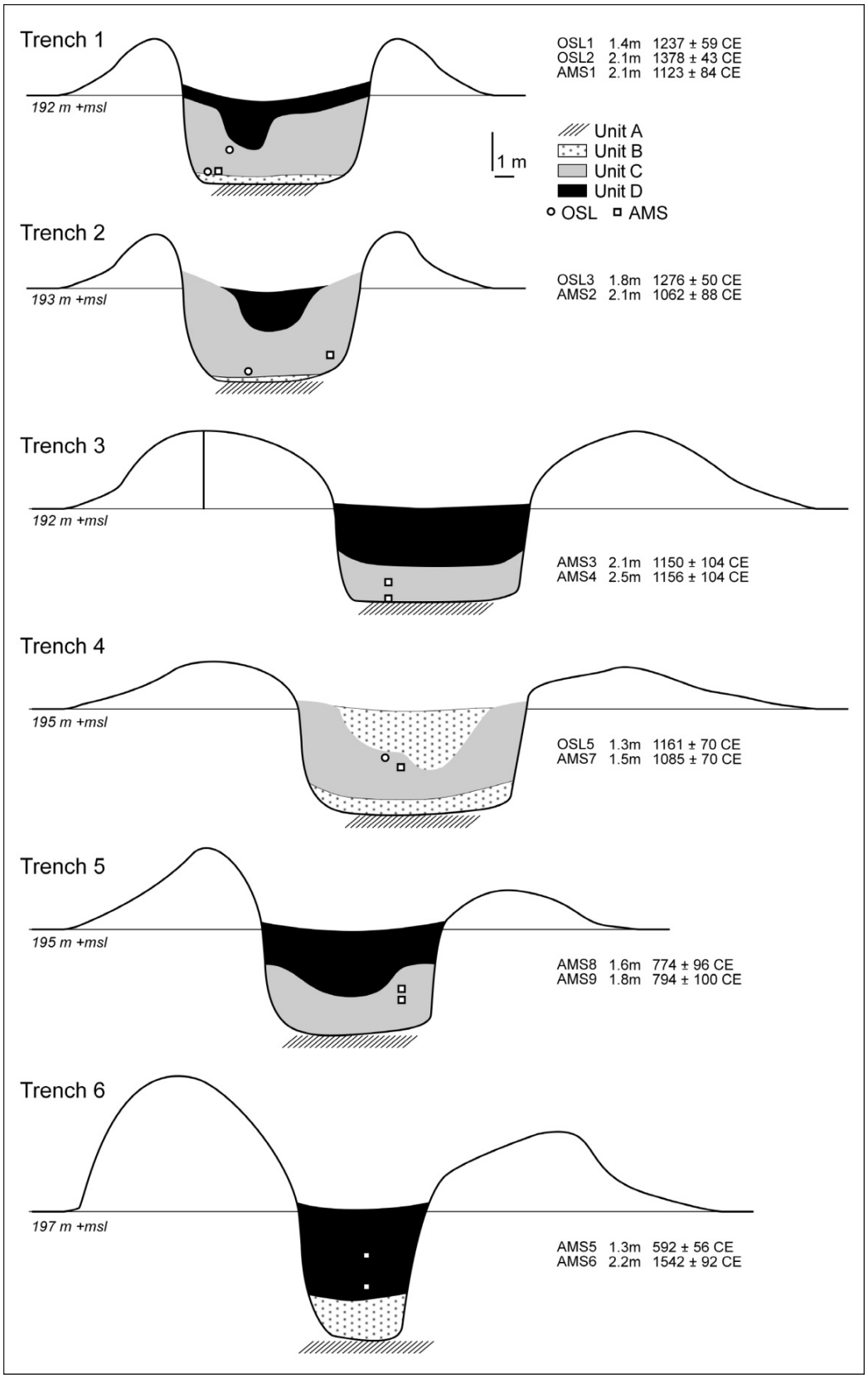

Figure S1: Geometry and sedimentary infill of investigated canals.

S2.2: Luminescence dating

Samples for luminescence dating were transferred to the Oxford Luminescence Dating Laboratory, University of Oxford, where they were opened and prepared under orange light conditions. Standard laboratory treatment was undertaken to isolate purified quartz grains, which included treatment

with hydrochloric acid and hydrogen peroxide to remove carbonate and organic matter, sieving, heavy liquid density separation and chemical etching with hydrofluoric acid to remove the alpha-irradiated outer layer of the quartz grains. Once prepared, very small aliquots (1 mm diameter) of sand sized quartz grains were prepared on aluminum discs.

Optically stimulated luminescence (OSL) measurements were made using a Risø TL/OSL luminescence reader fitted with a $^{90}Sr/^{90}Y$ beta source, which had a dose rate of approximately 4 Gy/min. Ultraviolet luminescence signals were stimulated with blue light emitting diodes (470 nm) and detected through a bialkali photo multiplier tube fitted with 7.5 mm U340 filters. Equivalent doses (D_e) were calculated using the single aliquot regenerative dose (SAR) protocol[25], using a pre-heat and cut-heat of 160°C for 10 s, selected following preheat and dose recovery tests. D_es were calculated from the background subtracted signal measured during the initial 0.1 s of stimulation. D_es were included in final age calculation if the following criteria were satisfied: 1) test dose signals >3σ background levels, 2) recuperation < 0.25 Gy; 3) recycling ratio and 4) OSL IR depletion ratio[26] within 10% of unity; 5) fast ratio >20[27]. Final D_e determinations (Tab. S1) were made using either the minimum age model (MAM)[28] or finite mixture model[29].

Environmental dose rates were calculated using DRAC (v1.2)[30]. To calculate the beta and gamma dose rates, radionuclide concentrations were converted into infinite-matrix dose rates[31] and adjusted for attenuation by grain size, chemical etching and a moisture content of 5 ± 2 %. Cosmic dose rates were calculated on the basis of geographic location and sample position[32]. Final age calculation was also undertaken in DRAC[30].

*Table S1: OSL dating summary. n refers to the number of small aliquots of quartz satisfying all rejection criteria and used for final D_e calculation (the number of measured aliquots are shown in parentheses). D_es were calculated using the minimum age model, apart from sample A3 (marked *) where the finite mixture model was used. All calculations were made prior to rounding.*

Sample	Grain size (µm)	n	Overdisper-sion (%)	Equivalent dose (Gy)	Dose rate (Gy.ka^{-1})	Age (ka)	Terrace/Trench sample depth (m)	Date
A1	210-250	54 (96)	92.9 ± 8.9	0.60 ± 0.08	2.28 ± 0.12	0.26 ± 0.04	Ta3 (0.8)	1755 ± 50 CE
A2	90-150	40 (48)	38.5 ± 3.3	0.72 ± 0.11	2.65 ± 0.14	0.27 ± 0.04	Ta3 (0.7)	1745 ± 40 CE
A3	90-150	60 (72)	60.9 ± 4.7	1.34 ± 0.19*	2.67 ± 0.14	0.50 ± 0.08	Ta3 (1.4)	1515 ± 80 CE *
A4	150-180	36 (48)	29.8 ± 2.5	5.51 ± 0.19	1.89 ± 0.11	2.91 ± 0.20	Ta2 (2.3)	895 ± 200 BCE
A5	150-180	45 (72)	43.4 ± 3.5	1.03 ± 0.11	2.30 ± 0.13	0.45 ± 0.05	Ta3 (1.3)	1565 ± 50 CE
A6	210-250	55 (72)	83.2 ± 7.7	1.00 ± 0.13	1.67 ± 0.10	0.60 ± 0.09	Ta3 (4.0)	1415 ± 90 CE
A7	150-180	60 (72)	133.7 ± 14.8	0.11 ± 0.02	2.39 ± 0.13	0.05 ± 0.01	Ta4 (0.9)	1965 ± 10 CE
A8	150-180	69 (120)	77.5 ± 6.1	1.50 ± 0.15	2.24 ± 0.13	0.67 ± 0.08	Ta2 (0.7)	1345 ± 80 CE
A9	210-250	55 (72)	56.3 ± 4.5	1.52 ± 0.14	2.20 ± 0.12	0.69 ± 0.36	Ta3 (2.3)	1325 ± 360 CE
A10	90-150	37 (48)	19.8 ± 1.7	24.53 ± 0.91	2.12 ± 0.11	11.58 ± 0.76	Ta1 (3.6)	9565 ± 760 BCE
B1	150-180	72 (96)	114.1 ± 10.5	0.48 ± 0.07	2.44 ± 0.13	0.20 ± 0.03	Tb3 (0.4)	1818 ± 30 CE
B2	150-180	63 (72)	25.2 ± 1.3	32.65 ± 2.45	1.90 ± 0.11	17.18 ± 1.63	Tb1 (6.2)	15165 ± 1630 BCE
B3	150-180	47 (72)	66.0 ± 5.8	3.09 ± 0.34	2.28 ± 0.12	1.35 ± 0.17	Tb4 (1.2)	665 ± 170 CE
B4	150-180	43 (48)	26.9 ± 2.0	27.68 ± 2.18	2.32 ± 0.12	11.94 ± 1.14	Tb1 (2.3)	9925 ± 1140 BCE
B5	150-180	32 (48)	21.2 ± 1.9	8.09 ± 0.31	2.45 ± 0.13	3.31 ± 0.21	Tb3 (4.2)	1295 ± 210 BCE
B6	150-180	41 (48)	10.6 ± 1.2	43.63 ± 2.19	2.36 ± 0.14	18.5 ± 1.41	Tb1 (5.8)	16485 ± 1410 BCE
B7	150-180	57 (72)	88.2 ± 8.0	1.94 ± 0.21	2.61 ± 0.13	0.74 ± 0.09	Tb5 (0.6)	1275 ± 90 CE
B8	150-180	35 (48)	26.5 ± 2.2	20.86 ± 1.58	2.77 ± 0.14	7.54 ± 0.69	Tb2 (2.7)	5525 ± 690 BCE
B9	210-250	49 (104)	46.5 ± 3.9	1.53 ± 0.16	2.31 ± 0.12	0.66 ± 0.08	Tb4 (2.0)	1355 ± 80 CE
B10	210-250	39 (72)	48.3 ± 4.3	2.82 ± 0.31	2.34 ± 0.13	1.21 ± 0.15	Tb4 (4.2)	805 ± 150 CE
OSL1	90-250	27 (64)	15.20 + 1.9	2.11 ± 0.10	2.71 ± 0.16	0.78 ± 0.06	Trench 1 (1.4)	1237 ± 59 CE
OSL2	180-210	32 (48)	9.29 + 1.7	1.77 ± 0.07	2.78 ± 0.15	0.64 ± 0.04	Trench 1 (2.1)	1378 ± 43 CE
OSL3	150-180	32 (48)	11.72 + 1.6	2.17 ± 0.08	2.93 ± 0.17	0.74 ± 0.05	Trench 2 (2.1)	1276 ± 50 CE
OSL4	180-210	30 (48)	21.88 + 2.1	3.33 ± 0.17	2.46 ± 0.14	1.35 ± 0.10	Trench 7 (3.0)	662 ± 100 CE
OSL5	125-180	54 (96)	30.04 + 2.9	2.42 ± 0.15	2.83 ± 0.17	0.86 ± 0.07	Trench 4 (1.3)	1161 ± 70 CE

References in Supplementary Materials

[1]G. Frumkin, Archaeology in Soviet Central Asia. E.J. Brill, Leiden/Köln (1970).

[2]V.H. Mair, The Bronze Age and Early Iron Age peoples of Eastern Central Asia. Institute for the Study of Man, Washington (1998).

[3]C.I. Beckwith, Empire of the Silk Road: A history of Central Eurasia from the Bronze Age to the present. Princeton University Press (2009).
[4]M.A. Dandamaev, A political history of the Achaemenid Empire. E.J. Brill, Leiden (1989).
[5]Y.G. Gulyamov, The history of irrigation of Khorezm from the ancient to present (in Russian). Academy of Sciences of the Soviet Uzbek Republic, Taskhkent, (1957), pp. 5-74.
[6]R.N. Frye, "Pre-Islamic and early Islamic cultures in Central Asia" in Turko-Persia in historical perspective, R.L. Canfield, Ed. (Cambridge University Press, 1991).
[7]E.V. Zeimal, "The Kidarite Kingdom in Central Asia" in History of Civilizations of Central Asia, volume 3: The crossroads of Civilization, A.D. 250-750, B.A. Litvinsky, Ed. (UNESCO Publishing, New York), pp. 123-137.
[8]A. Kurbanov, The Hephthalites: Archaeological and historical analysis. PhD thesis, Department of History and Cultural Studies of the Free University, Berlin.
[9]R. Grousset, The empire of the steppes: a history of Central Asia, Rutgers University Press (1970).
[10]P. Golden, An introduction to the history of the Turkic peoples: Ethnogenesis and state-formation in Medieval and Early Modern Eurasia and the Middle East. Otto Harrassowitz, Wiesbaden (1992).
[11]K. Baipakov, R. Nasirov. Along the Great Silk Road. Kramds-Reklama Yaynini, Alma-ata (1991).
[12]P. Wheatley, The Places Where Men Pray Together, Cities in Islamic Lands, Seventh through the Tenth Centuries. The University of Chicago Press, Chicago (2001).
[13]G. Dawkes, G. Jorayev, G., M. Macklin, W. Toonen, The form and abandonment of the city of Kuik-Mardan, Otrar oasis, Kazakhstan in the Early Islamic period. *J. Islam. Archaeol.* **6:2**, 137-152 (2020).
[14]E. Lioubimtseva, R. Cole, J.M. Adams, G. Kapustin, Impacts of climate and land-cover change in arid lands of Central Asia. *J. Arid Environ.* **62**, 285-308 (2005).
[15]F.H. Chen *et al.*, Moisture changes over the last millennium in arid central Asia: a review, synthesis and comparison with monsoon region. *Quat. Sci. Rev.* **29**, 1055-1068 (2010).
[16]I.P. Panyushkina, *et al.*, Runoff variations in Lake Balkhash Basin, Central Asia, 1779-2015, inferred from tree rings. *Clim. Dyn*. **51**, 3161-3177 (2018).
[17]P.O. Zavialov, Physical oceanography of the dying Aral Sea. Springer Verlag, Chichester (2005).
[18]T. Sato *et al.*, Water sources in semiarid northeast Asia as revealed by field observations and isotope transport model. *J. Geophys. Res.* **112**, D17112 (2007).
[19]E.M. Aizen, V.B. Aizen, J.M. Melack, T. Nakamura, T. Ohta, Precipitation and atmospheric circulation patterns at mid-latitudes of Asia. *Int. J. Climatol.* **21**, 535–556 (2001).
[20]Google Earth, Otrār Oasis, Kazakhstan. Maxar Technologies 2020. http://www.earth.google.com
[21]V. Groshev, Zimlidelie i irrigatsie yuzhne Kazakhstan i Semirechie (Agriculture and irrigation of South Kazakhstan and Semirechie), Alma-Ata (1986).
[22]L.E. Purdue, J.F. Berger, An integrated socio-environmental approach to the study of ancient water systems: the case of prehistoric Hohokam irrigation systems in semi-arid central Arizona, USA. *J. Archaeol. Sci.* **53**, 586-603 (2015).
[23]L. Cez, The Sarazm River and Irrigation Landscape in the Middle Zeravchan Valley, Tajikistan, Central Asia – Study of the Dynamics and Timelines of a Water Landscape in a Challenging Environment. Projets de paysage 20 (2019).
[24]W.H.J. Toonen, M.G. Kleinhans, K.M. Cohen, Sedimentary architecture of abandoned channel fills. *Earth Surf. Process. Landf.* **37:4**, 459-472 (2012).
[25]A.S. Murray, A.S., A.G. Wintle, A.G., Luminescence dating of quartz using an improved single-aliquot regenerative-dose protocol. *Radiat. Meas.* **32**, 57-73 (2000).
[26]G.A.T. Duller, Distinguishing quartz and feldspar in single grain luminescence measurements. *Radiat. Meas.* **37**, 161-165 (2003).
[27]J.A. Durcan, G.A.T. Duller, The fast ratio: a rapid measure for testing the dominance of the fast component in the initial OSL signal from quartz. *Radiat. Meas.* **46**, 1065-1072 (2011).
[28]R.F. Galbraith, G.M. Laslett, Statistical models for mixed fission track ages. *Nucl. Tracks Radiat. Meas.* **4**, 459-470 (1993).
[29]R.F. Galbraith, P.F. Green, Estimating the component ages in a finite mixture. *Nucl. Tracks Radiat. Meas.* **17**, 197-206 (1990).
[30]J.A. Durcan, G.E. King, G.E., G.A.T. Duller, DRAC: Dose rate and age calculator for trapped charge dating. *Quat Geochronol.* **28**, 54-61 (2015).
[31]G. Guerin, N. Mercier, G. Adamiec, Dose-rate conversion factors: update. *Ancient TL* **29**, 5-8 (2011).
[32]J.R. Prescott, J.T. Hutton, Cosmic Ray contributions to dose rates for luminescence and ESR dating: Large depths and long term variations. *Radiat. Meas.* **23**, 497-500 (2011).